J. Membrane Biol. 168, 131–139 (1999)

The Journal of
Membrane
Biology

Osmotic Shrinkage Activates Nonselective Cation (NSC) Channels in Various Cell Types

J.-P. Koch[1], **C. Korbmacher**[2]
[1]Zentrum der Physiologie, Johann Wolfgang Goethe-Universität, Theodor Stern Kai 7, D-60590 Frankfurt am Main, Germany
[2]University Laboratory of Physiology, Parks Road, Oxford, OX1 3PT UK

Received: 19 August 1998/Revised: 7 December 1998

Abstract. Osmotic cell shrinkage activates a nonselective cation (NSC) channel in M-1 mouse cortical collecting duct cells (Volk, Frömter & Korbmacher, 1995, *Proc. Natl. Acad. Sci. USA* **92:** 8478-8482). To see whether shrinkage-activated NSC channels are an ubiquitous phenomenon, we tested the effect of hypertonic extracellular solution on whole-cell currents of HT_{29} human colon carcinoma cells, BSC-1 renal epithelial cells, A10 vascular smooth muscle cells, and Neuro-2a neuroblastoma cells. Addition of 100 mM sucrose to an isotonic NaCl bath solution induced cell shrinkage of HT_{29} cells as evidenced by a decrease in cell diameter from 18 ± 1 μm to 12 ± 1 μm ($n = 13$). Upon cell shrinkage whole-cell currents of HT_{29} cells increased within 8 ± 1 min by about 30-fold ($n = 13$). Cell shrinkage and current activation were reversible upon return to isotonic solution. Replacement of bath Na^+ by K^+ or Li^+ had almost no effect on the stimulated inward current. In contrast, replacement by N-methyl-D-glucamine (NMDG) completely abolished it and shifted the reversal potential from −4.5 ± 0.7 mV to −57 ± 4.1 mV ($n = 10$). Thus, the stimulated conductance is nonselective for alkali cations but highly selective for cations over anions with a cation-to-anion permeability ratio of about 13. Flufenamic acid (100 μM) inhibited the stimulated current by 84 ± 4.7% ($n = 8$). During the early phase of hypertonic stimulation single-channel transitions could be detected in whole-cell current recordings, and a gradual activation of 12 and more individual channels with a single-channel conductance of 17.6 ± 0.9 pS ($n = 4$) could be resolved. In analogous experiments similar shrinkage-activated NSC channels were also observed in BSC-1 renal epithelial cells, A10 vascular smooth muscle cells, and Neuro-2a neuroblastoma cells. These findings indicate that shrinkage-activated NSC channels are an ubiquitous phenomenon and may play a role in volume regulation.

Key words: Cell shrinkage — Volume regulation — Patch clamp — Cell lines — Flufenamate — Cation channels

Introduction

In response to osmotic challenges most cells are able to activate volume regulatory mechanisms to reduce or increase cellular osmolyte content in order to avoid excessive cell swelling or cell shrinkage, respectively. Ions constitute the bulk of intracellular and extracellular osmolarity and ion transport across the cell membrane is the most efficient and rapid means of altering cellular osmolarity. During cell swelling, cells extrude ions to accomplish regulatory volume decrease (RVD), whereas during cell shrinkage, cells accumulate ions to achieve regulatory volume increase (RVI). Cell-volume regulation has been studied in many different cell types and several membrane transport processes involved in this regulation have been identified (for review: Lang et al., 1998). Cell swelling usually activates conductances for K^+ and Cl^-; the resulting KCl efflux inverts the osmotic gradient and the direction of H_2O flow. Cell shrinkage is known to activate electroneutral NaCl uptake mechanisms such as NaK-2Cl cotransport or Na^+/H^+ and parallel Cl^-/HCO^- exchanger. The mechanisms of activation of channels and transporters involved in volume regulation are not fully understood and are believed to involve a large number of signaling pathways.

Little is known about the involvement of ion channels in response to cell shrinkage. However, it has been reported that exposure to extracellular hypertonicity activates a nonselective cation conductance in lung alveo-

Correspondence to: C. Korbmacher

lar epithelial cells (Chan & Nelson, 1992) and in M-1 mouse cortical collecting duct cells. In M-1 cells the underlying shrinkage-activated nonselective cation (NSC) channel has been identified by single-channel recordings in the whole-cell configuration (Volk et al., 1995). Its single-channel conductance, ion selectivity, and inhibition by flufenamic acid suggest that the shrinkage-activated NSC channel is identical to the NSC channel previously characterized in inside-out patches of M-1 cells (Korbmacher et al., 1995). This NSC channel belongs to an emerging family of calcium-activated NSC channels which have been described in a large number of excitable and nonexcitable tissues (Siemen, 1993). A putative member of this channel family has recently been cloned (Suzuki et al., 1998).

These NSC channels are usually silent in cell-attached patches, and after patch excision require at least micromolar calcium concentrations at the cytosolic surface for activation. They are typically inhibited by cytosolic ATP concentrations in the millimolar range. Thus, a common problem with all members of this group is how these channels could be activated in a normal living cell. Indeed, the physiological role and mode of activation of the calcium-activated and ATP-inhibited NSC channels described in the literature is only poorly understood. The finding that cell shrinkage activated the NSC channel in M-1 cells suggested that this channel family may be involved in volume regulation. Therefore we hypothesised that NSC channels in other preparations may also be activated by cell shrinkage.

A calcium-activated and ATP-inhibited NSC channel similar to that found in M-1 cells has previously been identified in inside-out patches of HT_{29} human colon carcinoma cells a well-established model for the colonic crypt epithelial cell (Champigny, Verrier & Lazdunski, 1991). Thus, in the present study we investigated whether osmotic cell shrinkage would also activate the NSC channel in HT_{29} cells. Furthermore, to see whether shrinkage-activated NSC channels are an ubiquitous phenomenon, we tested the effect of hypertonic extracellular solution on whole-cell currents of BSC-1 renal epithelial cells, A10 vascular smooth muscle cells and Neuro-2a neuronal cells. The BSC-1 cell line derived from the African green monkey *C. aethiops* expresses properties typical for renal proximal tubular cells, namely an electrogenic $NaHCO_3$ symport (Jentsch et al., 1986). The A10 vascular smooth muscle cell line established from rat embryonic aorta maintains electrophysiolgical properties typical for vascular smooth muscle cells (Korbmacher et al., 1989). The Neuro-2a cell line derived from mouse neuroblastoma retains properties typical for neuronal cells including TTX-sensitive voltage gated Na^+ channels (Baumgarten et al., 1995). All four cell lines used in the present study have been widely used as model systems to study tissue specific membrane transport processes.

Materials and Methods

Cell Culture

The HT_{29} cell line (ATCC HTB-38) was kindly provided by Dr. G. Burckhardt, the A10 cell line (ATCC CRL-1476) and the Neuro-2a cell line (ATCC CCL-131) were a generous gift from Dr. T.J. Jentsch. The BSC-1 cell line (ATCC CCL-26) was from American Type Culture Collection (Rockville, MD). Cells were not tested for the presence of mycoplasmal contamination. BSC-1 and Neuro-2a cells were maintained in MEM medium supplemented with Earle's salts (Gibco-BRL/Life Technologies, Eggenstein, Germany); A10 cells and HT_{29} cells were maintained in DMEM medium (Seromed/Biochrom KG, Berlin, FRG). All media were supplemented with 2 mM glutamine, 100 U/ml penicillin, 100 μg/ml streptomycin. The media for HT_{29}, BSC-1 and Neuro-2a cells contained 10% fetal calf serum, the medium for A10 cells contained 20% fetal calf serum (Seromed/Biochrom KG, Berlin, FRG). Moreover, the media for A10 cells and Neuro 2a cells were supplemented with 1% (v/v) nonessential amino acid solution (100×; Gibco BRL/Life Technologies, Eggenstein, FRG). Cells were passaged with a split ratio of about 1:5 using 0.05% Trypsin/0.02% EDTA (w/v) in calcium- and magnesium-free PBS (Seromed/Biochrom KG, Berlin, FRG). Cells were routinely grown on uncoated tissue culture dishes (Becton Dickinson, Plymouth, England) and maintained in a 5% CO_2 atmosphere at 37°C. For patch-clamp experiments cells were seeded onto small pieces of glass coverslips and were used one day after seeding. BSC-1 cells were used 1–3 days after seeding.

Patch Clamp Technique

The ruptured-patch whole-cell configuration of the patch clamp technique was used (Hamill et al., 1981) and experimental procedures were essentially as described previously (Letz et al., 1995; Volk et al., 1995). Experiments were performed at room temperature. An EPC-9 patch clamp amplifier (HEKA Elektronik, Lambrecht, Germany) was used to measure whole-cell currents or membrane voltage (V_m). An ATARI computer system was used to operate the EPC-9 amplifier and for data acquisition and analysis. Cells were viewed through a 40× objective of a Nikon TMS inverted microscope (Nikon GmbH, Düsseldorf, Germany) equipped with Hoffman modulation optics (Modulation Optics, Greenvale, NY) and cell diameter was estimated using a micrometer grid. Patch pipettes were pulled from Clark glass capillaries (Clark Electromedical Instruments, Pangbourne, UK) and had a resistance of 3.3 ± 0.1 MΩ (n = 52) in NaCl/Ringer when filled with NaCl/EGTA pipette solution (*see below*). The reference electrode was an Ag/AgCl pellet bathed in the same solution as that used in the pipette, and connected to the bath via an agar/pipette-solution bridge in the outflow path of the chamber. Liquid junction (LJ) potentials occurring at the bridge/bath junction were measured using a 3M KCl flowing boundary electrode and ranged from −3 mV to +4 mV. For data analysis the V_{pip} values were corrected accordingly while the original traces shown in the figures are not LJ corrected. Upward (positive) current deflections correspond to cell membrane outward currents. The membrane capacitance (C_m) and series resistance (R_s) were estimated by nulling capacitive transients using the automated EPC-9 compensation circuit. In HT_{29} cells, BSC-1 cells, A10 cells, and Neuro-2a cells C_m averaged 14 ± 1.6 pF (n = 15), 10 ± 0.7 pF (n = 16), 43 ± 3.9 pF (n = 11), and 17 ± 1.4 pF (n = 10), respectively. The corresponding R_s values averaged 10 ± 0.9 MΩ (n = 15), 10 ± 0.8 MΩ (n = 16), 9 ± 1.3 MΩ (n = 11), and 11 ± 1.2 MΩ (n = 10); R_s was not compensated. For data analysis the current data were filtered at 200 Hz and were read into the computer via the ITC-16 interface of the EPC-9 patch clamp am-

plifier at a sample rate of 1 kHz. Single channel current amplitudes were estimated from amplitude histograms. Pulsed current data were analyzed using the 'Review'-program (Instrutech, Elmont, NY) and continuous current data were analyzed using our own software written by A. Rabe. Data are given as mean values ± SEM, significances were evaluated by the appropriate version of Student's *t*-test.

Solutions and Chemicals

The standard bath solution was NaCl-solution (in mM): 140 NaCl, 5 KCl, 1 $CaCl_2$, 1 $MgCl_2$, and 10 Hepes (adjusted to pH 7.5 with NaOH). For testing monovalent cation selectivity the Na^+ was replaced by an equal amount of K^+, Li^+ or NMDG (N-methyl-D-glucamine). All bath solutions contained 5 mM glucose. Extracellular hyperosmolarity was achieved by adding 100 mM sucrose to the bath solution without changing its ionic composition. Pipettes were filled with NaCl/EGTA-solution (in mM: 145 NaCl, 1 EGTA, 1 $MgCl_2$, 10 Hepes adjusted to pH 7.5 with NaOH). Flufenamic acid was purchased from Sigma (Deisenhofen, Germany) and was directly dissolved in bath solution on the day of the experiment.

Results

Effect of Extracellular Hypertonicity on HT_{29} Whole-Cell Currents

The effect of extracellular hypertonicity on HT_{29} whole-cell currents was investigated in experiments as shown in Fig. 1*A*. Under isotonic control conditions at a holding potential of −40 mV inward currents were small, and replacement of Na^+ in the bath by the impermeable cation NMDG had almost no effect on the inward current. However, about three minutes after changing to hypertonic bath solution the inward current markedly increased and replacement of Na^+ with NMDG completely abolished the stimulated inward current. This indicated that the stimulated inward current was carried by Na^+. After about 6 min the current stimulation and the NMDG effect reached a maximum. In similar experiments summarized in Fig. 1*B* hypertonicity reversibly increased the inward current about 30-fold from −6 ± 2 pA to −186 ± 28 pA ($n = 13$). In these experiments onset of current stimulation was observed 3 ± 1 min after changing to hypertonic bath solution and reached its maximum after 8 ± 1 min ($n = 13$). As shown in Fig. 1*C* and 1*D* there is a reciprocal change in cell diameter and whole-cell current with diameter change preceding current change. On average cell diameter decreased from 18 ± 1 μm under control conditions to 12 ± 1 μm in the presence of 100 mM sucrose ($n = 13$). As shown in Fig. 1 *A* current stimulation was reversible after returning to isotonic bath solution. In 8 out of 13 experiments seals could be maintained long enough to observe recovery back to baseline current levels (Fig. 1 *B*) which was completed within 4 ± 0.3 min after washout of the hypertonic bath solution. The cell diameter recovered from 13 ± 1 back to 15 ± 1 μm ($n = 8$). As shown in Fig. 1*A* application of 100 μM flufenamic acid, a derivative of the Cl^- channel blocker DPC and potent blocker of NSC channels (Gögelein et al., 1990; Gögelein and Pfannmüller, 1989), largely inhibited the hypertonicity-stimulated inward currents, on average by 84 ± 5% ($n = 8$, $P < 0.001$).

Selectivity of the Stimulated Whole Cell Current

The cation selectivity of the stimulated whole-cell current was investigated in experiments as shown in Fig. 2*A*. During maximal stimulation of whole-cell currents in hypertonic solution (NaCl solution with 100 mM sucrose) bath Na^+ was replaced by the monovalent cations K^+ or Li^+. As shown before, Na^+ replacement by NMDG completely abolished the inward current under these conditions, whereas replacement by K^+ and Li^+ only slightly reduced the inward currents. This indicates that the stimulated ion channels discriminate poorly among these alkali cations. Results from similar experiments are summarized in Fig. 2*B*. Figure 3 shows individual whole-cell current traces (Fig. 3*A*) and corresponding *I/V*-plots (Fig. 3*B*) obtained from voltage step protocols applied during a similar experiment as shown in Fig. 1*A*. The stimulated currents did not exhibit any major voltage-dependent activation or inactivation when voltage pulses of 400 msec duration were applied between −120 and +120 mV (Fig. 3*A*). However, the *I/V*-relationship of the stimulated current was slightly outwardly rectifying (Fig. 3*B*) which suggests that the underlying channels may have a slightly higher open probability at depolarizing voltages which is a characteristic feature of nonselective cation channels (Korbmacher et al., 1995). Under stimulated conditions replacement of extracellular Na^+ with NMDG shifted the reversal potential from −4.5 ± 0.7 mV to −57 ± 4.1 mV ($n = 10$) which is compatible with the observation of a small outward current in the presence of NMDG observed at a holding potential of −40 mV (Fig. 1). Taken together, these findings indicate, that the stimulated channel discriminates poorly between Na^+, K^+ and Li^+, but is highly selective for cations over anions with a cation-to-chloride permeability ratio of about 13.

Identification of the Single Channels Underlying the Hypertonicity-Induced Nonselective Cation Conductance

Under physiological conditions the whole-cell conductance of HT_{29} cells is dominated by a K^+ conductance (Bajnath et al., 1991). Under our experimental conditions with symmetrical NaCl solutions in bath and pipette this K^+ conductance is basically eliminated. Thus, the overall cell conductance measured under isotonic

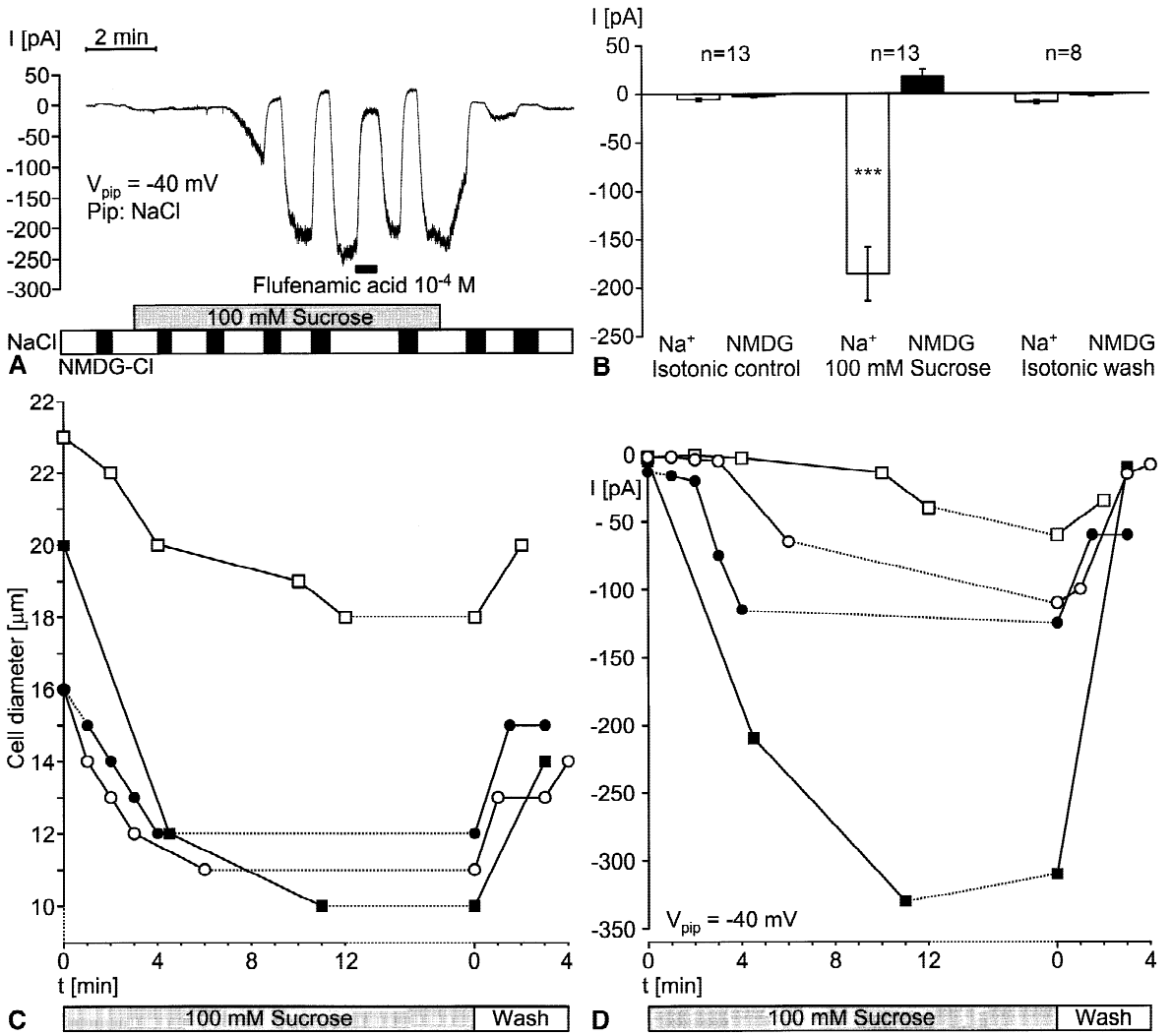

Fig. 1. Extracellular hypertonicity activates a Na^+ inward current in HT_{29} cells which is inhibited by flufenamic acid. (*A*) The continuous whole-cell current trace was recorded at a pipette potential (V_{pip}) of −40 mV. Pipette was filled with NaCl/EGTA solution and bath was initially isotonic NaCl solution. Bars indicate extracellular Na^+ replacement by NMDG, presence of 100 mM sucrose, and application of 10^{-4} M flufenamic acid. (*B*) Bar diagram summarizes whole-cell current data obtained during similar experiments as in *A*. Open and black columns represent currents measured in the presence or absence of Na^+ (replaced by NMDG), respectively. Measurements were obtained during isotonic conditions (isotonic control), during hypertonic conditions (100 mM sucrose), and after washout of sucrose (isotonic wash). Numbers of experiments (*n*) and SEM values (error bars) are indicated. In the presence of Na^+ application of 100 mM sucrose significantly increases the inward current (*** $P \leqslant 0.001$, paired *t*-test). In (*C*) and (*D*) changes in cell diameter and whole-cell inward current are compared during exposure to hypertonic bath solution and subsequent washout. Data from four individual experiments are shown and different symbols are used for the different experiments to indicate corresponding cell diameter and whole-cell current data (*I*).

conditions is small. At a holding potential of −40 mV inward currents averaged −6.7 pA which corresponds to an initial input resistance of about 6 GΩ. We have previously shown that under these conditions it is possible to resolve single channel current transitions in the whole-cell configuration (Volk et al., 1995). In order to identify the single-channels that are activated during cell shrinkage we focused our attention on the initial phase of the current activation after changing to hypertonic bath solution (Fig. 4*A*). Figure 4*B* shows an example of such a whole-cell current trace recorded three minutes after changing to hypertonic bath solution. At this resolution single-channel transitions can be resolved. The number of active single channels increased continuously throughout the recording with prolonged hypertonic stimulation. The current amplitude histogram of the current trace shows 12 equidistant peaks which correspond to the open and closed levels of single-channels that were activated in the cell membrane. The single-channel current amplitude was 0.78 pA. At a holding potential of

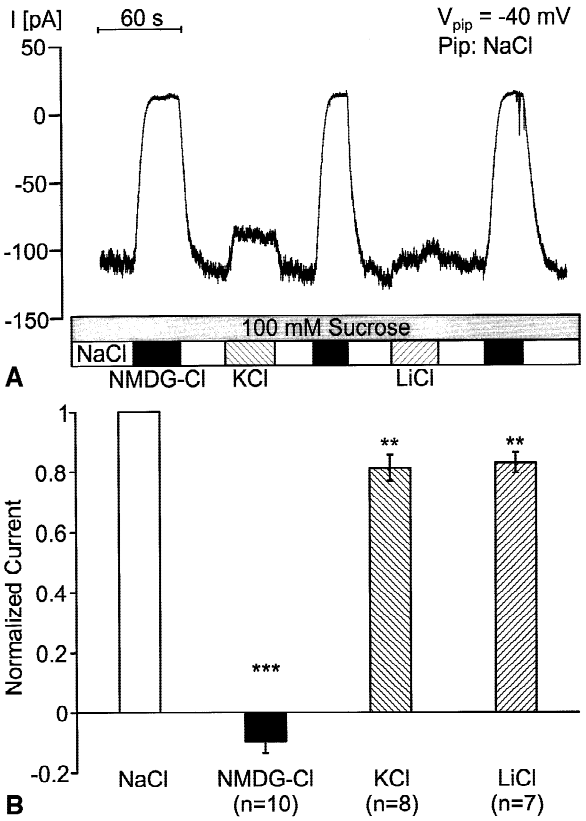

Fig. 2. Monovalent cation selectivity of hypertonicity-activated whole-cell current in HT_{29} cells. (*A*) Experimental conditions were the same as in Fig. 1. During maximal hypertonic activation of whole-cell currents extracellular Na^+ was replaced by NMDG, K^+, or Li^+ in the continuous presence of 100 mM sucrose as indicated below the trace. (*B*) Bar diagram summarizes results from similar experiments as shown in *A*. In each experiment currents were normalized to the hypertonicity activated inward current in the presence of Na^+. Number of experiments (*n*), SEM values (error bars) and significances are indicated (** $P \leq 0.01$; *** $P \leq 0.001$, paired *t*-test).

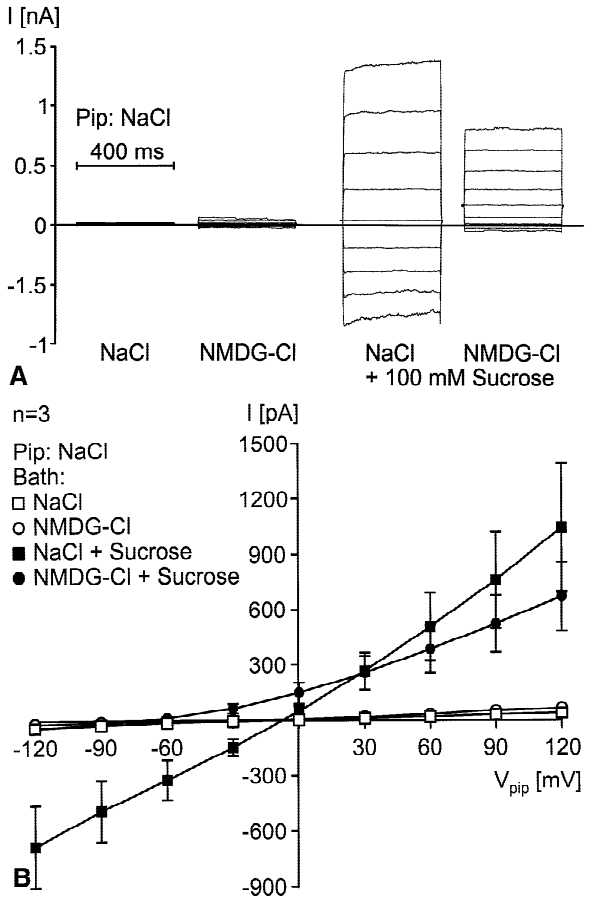

Fig. 3. Individual whole-cell current traces (*A*) obtained in HT_{29} cells from voltage-step protocols in the presence and absence of extracellular Na^+ (replaced by NMDG) before and after changing to a hypertonic bath solution (100 mM sucrose). From a holding potential (V_{pip}) of 0 mV voltage pulses of 400 msec duration were applied between −120 and +120 mV (in 30 mV increments). The pipette was filled with NaCl/EGTA solution. In (*B*) corresponding *I/V* plots are shown. Data were obtained from three similar experiments as depicted in *A*. Vertical bars indicate SEM values.

−40 mV this corresponds to a single-channel conductance of 19.5 pS. During further exposure to hypertonic bath solution the whole-cell currents continued to increase and eventually reached a maximum of about 280 pA (*not shown*), but single-channel events could no longer be resolved once the current exceeded approximately −20 pA. After returning to isotonic solution, however, when the stimulated current gradually declined below –20 pA, the same type of current transitions could again be resolved (*not shown*). In 4 such experiments the single-channel conductance of the activated NSC channels averaged 17.6 ± 0.9 pS.

Effect of Hypertonicity on BSC-1 Cells, A10 Cells and Neuro 2a Cells

Similar experiments as described above for the HT_{29} cells were also performed in BSC-1 cells, A10 cells and Neuro 2a cells. Hypertonicity activated a nonselective cation conductance in all three cell lines and the underlying single channels could be identified. Results are summarized in the Table which also contains corresponding data obtained in M-1 cells (Volk et al., 1995) for comparison. All channels activated by cell shrinkage in the various cell types discriminated poorly between Na^+ and K^+. However, the slightly different permeability ratio P_{Na}/P_K of the channel in Neuro-2a cells and the range of single channel conductances observed in the different cell types (15 to 27 pS) may indicate that different tissues express similar but not identical nonselective cation channels.

Discussion

This study demonstrates that osmotic cell shrinkage activates a nonselective cation conductance in cultured

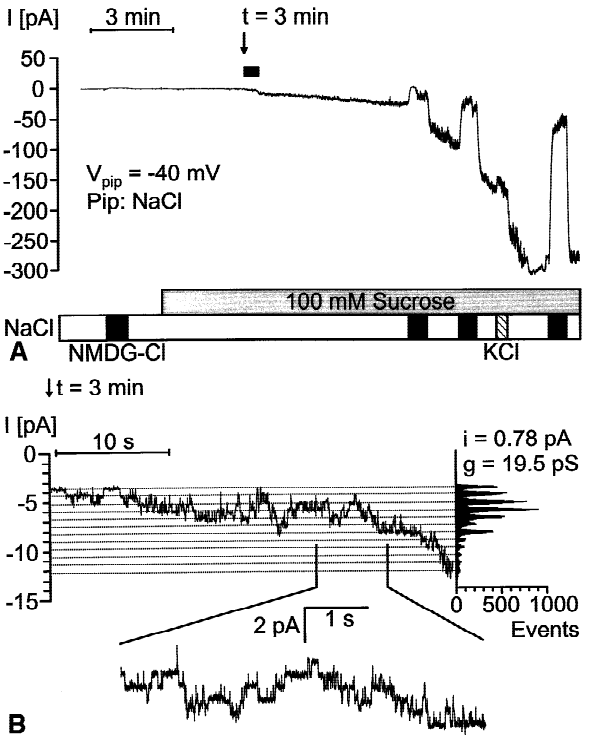

Fig. 4. Detection of single-channel current transitions in a whole-cell recording of a HT_{29} cell during the initial phase of current activation by hypertonicity. Experimental conditions were the same as in Fig. 1. The whole-cell current trace in (*A*) gives an overview of the current activation by hypertonicity. The bath solution exchanges (indicated below the trace) confirm that the stimulated current is largely abolished by removal of extracellular Na^+ (replaced by NMDG) and may be carried by K^+. The portion of the current trace indicated by the black bar above the trace at 3 minutes ($t = 3$ min) after application of 100 mM sucrose is enlarged in (*B*). A current-amplitude histogram of this portion was obtained and is shown to the right. Lines correspond to peaks of the histogram. The inset below demonstrates current transitions at expanded scales.

cells derived from a variety of tissues including colonic and renal epithelia, aortic vascular smooth muscle, and neuroblastoma tissue. The activated channels are highly selective for cations over anions but discriminate poorly between Na^+ and K^+. They are inhibited by flufenamic acid and have a single-channel conductance ranging from 15 to 27 pS.

Shrinkage-Activated NSC Channel and Calcium-Activated NSC Channel

The findings of our present study are reminiscent of previous reports of shrinkage-activated nonselective cation conductances in airway epithelial cells (Chan & Nelson, 1992) and in M-1 mouse cortical collecting duct cells (Volk et al., 1995). In M-1 cells the shrinkage-activated nonselective cation channel appears to be identical to a calcium-activated and ATP-inhibited NSC channel previously identified in inside-out patches of M-1 cells (Korbmacher et al., 1995). A similar calcium-activated NSC channel has also been identified in inside-out patches of HT_{29} human colon carcinoma cells (Champigny et al., 1991) and also in the basolateral membrane of rat colonic crypt base cells (Bleich et al., 1996). Its single-channel conductance, ion-selectivity and sensitivity to flufenamic acid suggest that the shrinkage-activated channel identified in our present study is identical to the calcium-activated NSC channel previously described in inside-out patches of HT_{29} cells. However, the activation mechanism is probably quite different in the inside-out and the whole-cell configuration (*see below*).

Similar calcium-activated NSC channels have been reported in a large number of preparations (Siemen, 1993) including neuroblastoma cells (Yellen, 1982), vascular smooth muscle cells (Wang, Hogg & Large, 1993), renal proximal tubule cells (Chraibi et al., 1994), and airway epithelial cells (Orser et al., 1991). Thus, we may speculate that calcium-activated NSC channels correspond to the shrinkage-activated NSC channels in Neuro-2a, A10, and BSC-1 cells identified in our present study and possibly to the channels underlying the shrinkage-activated nonselective cation conductance previously reported in airway epithelial cells (Chan & Nelson, 1992). Interestingly, calcium-activated NSC channels are usually quiescent and not detectable in cell-attached patches. So far their physiological role in the various tissues remains somewhat unclear (Siemen, 1993; Korbmacher & Barnstable, 1993). Our findings indicate that cell shrinkage may be a physiological stimulus for the activation of these ubiquitously expressed channels.

Mechanism of Channel Activation

Interestingly, in the whole-cell configuration shrinkage activation of the channel does not seem to require an increase in the intracellular calcium concentration and is not prevented by millimolar cytosolic ATP (Volk et al., 1995). This agrees well with the generally accepted view that intracellular calcium signaling plays an important role for volume regulation during hypotonic cell swelling but is not important during hypertonic cell shrinkage (McCarty & O'Neil, 1992). Thus, channel activation in excised inside-out patches by at least micromolar cytosolic calcium in the absence of cytosolic ATP probably does not reflect the physiologically relevant activation mechanism. Exposure to hypertonic solutions causes cell shrinkage. Thus, mechanical transduction mechanisms within the cell membrane or involving the cytoskeleton may contribute to activation of the NSC channel. A direct interaction of the cytoskeleton with ion channels has been discussed for a number of different

Table. Comparison of shrinkage-activated nonselective cation channels in various cell types

Cell Type	Origin	*I_{NSC} at V_{pip} = −40 mV		P_{Na}/P_K	Inhibition by Flufenamate	Single channel conductance [pS]
		Control [pA]	100 mM Sucrose [pA]HT29			
HT_{29}	Human colon carcinoma	3.5 ± 1.1	203 ± 31 (n = 13)	1/0.82	84 ± 5% (n = 8)	17.6 ± 0.9 (n = 4)
BSC-1	Africa green monkey kidney	1.7 ± 0.2	50 ± 15 (n = 15)	1/0.84	95 ± 1% (n = 3)	15.1 ± 0.3 (n = 4)
A10	Embryonic rat aorta	18.0 ± 6.1	521 ± 127 (n = 7)	1/0.85	93 ± 2% (n = 7)	27.2 ± 0.7 (n = 3)
Neuro-2a	Mouse neuroblastoma	6.0 ± 1.3	181 ± 56 (n = 7)	1/1.17	46 ± 4% (n = 4)	24.1 ± 0.7 (n = 4)
§M-1	Mouse cortical collecting duct	6.7 ± 1.2	235 ± 12 (n = 103)	1/0.90	84 ± 6% (n = 3)	26.7 ± 0.4 (n = 29)

* I_{NSC} was calculated by subtracting the whole-cell current measured in the presence of NaCl from the whole-cell current in the presence of NMDG-Cl.
§ Data obtained in M-1 cells (Volk et al., 1995) are included for comparison.

channels (Janmey, 1998). Involvement of the cytoskeleton could explain the different Ca^{2+} sensitivities of channels in the whole-cell configuration and in inside-out patches because patch excision may affect cytoplasmic regulatory sites by disrupting the cytoskeleton below the cell membrane (Milton & Caldwell, 1990). In contrast, in the whole-cell configuration the local damage to the cytoskeleton around the patch pipette is negligible and does not prevent channel activation in the rest of the cell membrane. Preliminary experiments performed in M-1 cells suggest that preincubation of M-1 cells with cytochalasin D, an agent that disrupts the cytoskeleton, reduces the whole-cell current response to cell shrinkage by about 70% (J.-P. Koch, *unpublished observation*). This finding supports the interpretation that an intact cytoskeleton is needed to mediate shrinkage activation of the nonselective cation channel. The activation mechanism may be even more complex involving additional regulatory proteins and phosphorylation steps (Nelson et al., 1996). In this context it is of interest that osmotic cell shrinkage triggers the expression of several proteins involved in the mitogen-activated protein (MAP) kinase pathway (Lang et al., 1998). Moreover, transcription of a serine/threonine kinase has been shown to be activated by cellular shrinkage and therefore may contribute to physiological responses to osmotic stress (Waldegger et al., 1997).

Physiological Role of the Shrinkage-Activated NSC Channel

Its activation by extracellular hypertonicity suggests that the NSC channel participates in the regulatory response to osmotic cell shrinkage. Indeed, it has been suggested that in some cells electrolyte accumulation during regulatory volume increase (RVI) may be accomplished by activation of Na^+ channels and/or nonselective cation channels (Chan & Nelson, 1992; Volk et al., 1995; Wehner et al., 1995). Under physiological conditions opening of NSC channels by cell shrinkage causes influx of Na^+ ions and depolarises the cell. For conductive Na^+ entry to mediate RVI, a parallel anion uptake is required and depolarisation of the cell membrane favors such conductive Cl^- entry. Under our experimental conditions we did not observe a shrinkage activation of a Cl^- conductance but the intrinsic Cl^- conductance of the cells may be sufficient to balance electrogenic Na^+ entry under hypertonic stress resulting in quasi-electroneutral uptake of Na^+ and Cl^-. The increase in cell Na^+ in turn activates the Na^+/K^+ ATPase which results in an increase in cell K^+. By this sequence of events a shrinkage-activated NSC may contribute to RVI. On the other hand, influx of Na^+ ions and cell depolarization may trigger or modulate intracellular signaling pathways like the MAP kinase cascade. Thus, activation of NSC channels may be an early signal for the regulation of ion transporters or metabolic pathways involved in volume regulation in response to cellular shrinkage.

In contrast to our findings in HT_{29} cells it has recently been reported that hypertonic cell shrinkage does not activate a nonselective cation channel in rat colonic crypt cells (Weyand et al., 1998) which are known to express calcium-activated NSC channels in excised inside-out patches similar to those found in HT_{29} cells (Bleich et al., 1996). We have no obvious explanation for this discrepant finding. However, the functional state of colonic crypt cells from freshly isolated tissue is likely to be different than in cultured HT_{29} cells. Indeed, so far shrinkage activated NSC cells have been exclusively detected in cultured cells. These cultured cells express tissue specific properties typical for the tissues of their origin. However, they are rapidly proliferating and not

fully differentiated cells. This suggests that the shrinkage-activated NSC channel may be particularly important during cell proliferation (Jung, Selvaraj & Gargus, 1992) which is known to involve changes in cell volume (Lang et al., 1998). On the other hand, one of the hallmarks of apoptotic cell death is cell shrinkage and doubling of extracellular osmolarity has been shown to trigger apoptosis (Bortner & Cidlowski, 1996; Matthews and Feldman, 1996). Moreover, it has been suggested that changes in ion channel activities may be involved in the early phase of apoptosis (Beauvais, Michel & Dubertret, 1995; Nagy et al., 1995). Clearly, the role of cell volume regulatory mechanisms in apoptotic cell death is still ill-defined (Lang et al., 1998). However, the importance of cell shrinkage for the apoptotic process suggests that the shrinkage-activated NSC channel may play a role in apoptosis which would possibly explain its ubiquitous expression.

We conclude that activation of NSC channels by cell shrinkage is a phenomenon that may be observed in various cell types of epithelial and nonepithelial origin. This is reminiscent of the ubiquitously expressed swelling-activated Cl^- channel (Strange, Emma & Jackson, 1996; Okada, 1997) and may indicate that the shrinkage-activated NSC is its functional counterpart. The molecular nature of the shrinkage-activated NSC channel is presently unknown but it may belong to the family of calcium-activated ATP-sensitive NSC channels previously identified in excised inside-out patches of numerous preparations.

The expert technical assistance of U. Fink and I. Doering-Hirsch is gratefully acknowleged. We thank A. Rabe for programming the computer software. This work was supported by a grant from the Deutsche Forschungsgemeinschaft (DFG grant Fr 233/9-1 and Ko 1057/7-1) and the Wellcome Trust.

References

Bajnath, R.B., Augeron, C., Laboisse, C.L., Bijman, J., de Jonge, H.R., Groot, J.A. 1991. Electrophysiological studies of forskolin-induced changes in ion transport in the human colon carcinoma cell line HT-29 cl.19A: Lack of evidence for a cAMP-activated basolateral K^+ conductance. *J. Membrane Biol.* **122:**239–250

Baumgarten, C.M., Dudley, S.C. Jr., Rogart, R.B., Fozzard, H.A. 1995. Unitary conductance of Na^+ channel isoforms in cardiac and NB2a neuroblastoma cells. *Am. J. Physiol.* **269:**C1356–C1363

Beauvais, F., Michel, L., Dubertret, L. 1995. Human eosinophils in culture undergo a striking and rapid shrinkage during apoptosis. Role of K^+ channels. *J. Leukocyte Biol.* **57:**851–855

Bleich, M., Riedemann, N., Warth, R., Kerstan, D., Leipziger, J., Hör, M., Van Driessche, W., Greger, R. 1996. Ca^{2+}-regulated K^+ and nonselective cation channels in the basolateral membrane of rat colonic crypt base cells. *Pfluegers Arch.* **432:**1011–1022

Bortner, C.D., Cidlowski, J.A. 1996. Absence of volume regulatory mechanisms contributes to the rapid activation of apoptosis in thymocytes. *Am. J. Physiol.* **271:**C950–C961

Champigny, G., Verrier, B., Lazdunski, M. 1991. A voltage, calcium, and ATP sensitive non selective cation channel in human colonic tumor cells. *Biochem. Biophys. Res. Comm.* **176:**1196–1203

Chan, H.C., Nelson, D.J. 1992. Chloride-dependent cation conductance activated during cellular shrinkage. *Science* **257:**669–671

Chraibi, A., Van den Abbeele, T., Guinamard, R., Teulon, J. 1994. A ubiquitous nonselective cation channel in the mouse renal tubule with variable sensitivity to calcium. *Pfluegers Arch.* **429:**90–97

Gögelein, H., Pfannmüller, B. 1989. The nonselective cation channel in the basolateral membrane of rat exocrine pancreas. *Pfluegers Arch.* **413:**287–298

Gögelein, H., Dahlem, D, Englert, H.C., Lang, H.J. 1990. Flufenamic acid, mefenamic acid and niflumic acid inhibit single nonselective cation channels in the rat exocrine pancreas. *FEBS. Lett.* **268:**79–82

Hamill, O.P., Marty, A., Neher, E., Sakmann, B., Sigworth, F.J. 1981. Improved patch clamp techniques for high-resolution current recording from cells and cell-free membrane patches. *Pfluegers Arch.* **391:**85–100

Janmey, P.A. 1998. The Cytoskeleton and cell signaling: component localization and mechanical coupling. *Physiol. Rev.* **78:**763–781

Jentsch, T.J., Matthes, H., Keller, S.K., Wiederholt, M. 1986. Electrical properties of sodium bicarbonate symport in kidney epithelial cells (BSC-1). *Am. J. Physiol.* **251:**F954–F968

Jung, F., Selvaraj, S., Gargus, J.J. 1992. Blockers of platelet-derived growth factor-activated nonselective cation channel inhibit cell proliferation. *Am. J. Physiol.* **262:**C1464–C1470

Korbmacher, C., Barnstable, C.J. 1993. Renal epithelial cells show nonselective cation channel activity and express a gene related to the cGMP-gated photoreceptor channel. *In:* Nonselective cation channels: Pharmacology, Physiology and Biophysics. D. Siemen and J. Hescheler, editors. pp. 147–164. Birkhäuser Verlag, Basel, Switzerland

Korbmacher, C., Helbig, H., Stahl, F., Coroneo, M., Haller, H., Lindschau, C., Quass, P., Wiederholt, M. 1989. Continuous membrane voltage recordings in A10 vascular smooth muscle cells: effect of AVP. *Am. J. Physiol.* **257:**C323–C332

Korbmacher, C., Volk, T., Segal, A.S., Boulpaep, E.L., Frömter, E. 1995. A calcium-dependent nucleotide-sensitive nonselective cation channel in M-1 mouse cortical collecting duct cells. *J. Membrane Biol.* **146:**29–45

Lang, F., Busch, G.L., Ritter, M., Völkl, H., Waldegger, S., Gulbins, E., Häussinger, D. 1998. Functional significance of cell volume regulatory mechanisms. *Physiol. Rev.* **78:**247–306

Letz, B., Ackermann, A., Canessa, C.M., Rossier, B.C., Korbmacher, C. 1995. Amiloride-sensitive sodium channels in confluent M-1 mouse cortical collecting duct cells. *J. Membrane Biol.* **148:**127–141

Matthews, C.C., Feldman, E.L. 1996. Insulin-like growth factor I rescues SH-SY5Y human neuroblastoma cells from hyperosmotic induced programmed cell death. *J. Cell Physiol.* **166:**323–331

McCarty, N.A., O'Neil, R.G. 1992. Calcium signaling in cell volume regulation. *Physiol. Rev.* **72:**1037–1061

Milton, R.L, Caldwell, J.H. 1990. How do patch clamp seals form? A lipid bleb model. *Pfluegers Arch.* **416:**758–765

Nagy, P., Panyi, G., Jenei, A., Bene, L., Gaspar, R., Matko, J., Damjanovich, S. 1995. Ion-channel activities regulate transmembrane signalling in thymocyte apoptosis and T-cell activation. *Immunology Letters* **44:**91–95

Nelson, D.J., Tien, X.-Y., Xie, W., Brasitus, T.A., Kaetzel, M.A., Dedman, J.R. 1996. Shrinkage activates a nonselective conductance: involvement of a Walker-motif protein and PKC. *Am. J. Physiol.* **270:**C179–191

Okada, Y. 1997. Volume expansion-sensing outward-rectifier Cl^- channel: fresh start to the molecular identity and volume sensor. *Am. J. Physiol.* **273:**C755–C789

Orser, B., Bertlik, M., Fedorko, L., O'Brodovich, H. 1991. Cation selective channel in fetal alveolar type II epithelium. *Biochim. Biophys. Acta* **1094:**19–26

Siemen D. 1993. Nonselective cation channels. *In:* Nonselective Cation Channels: Pharmacology, Physiology and Biophysics. D. Siemen and J. Hescheler, editors. pp. 3–25. Birkhäuser Verlag, Basel, Switzerland

Strange, K., Emma, F., Jackson, P.S. 1996. Cellular and molecular physiology of volume-sensitive anion channels. *Am. J. Phyisol.* **270:**C711–C730

Suzuki, M., Murata, M., Ikeda, M., Miyoshi, T., Imai, M. 1998. Primary structure and functional expression of a novel nonselective cation channel. *Biochem. Biophys. Res. Commun.* **242:**191–196

Volk, T., Frömter, E., Korbmacher, C. 1995. Hypertonicity activates nonselective cation channels in mouse cortical collecting duct cells. *Proc. Natl. Acad. Sci. USA* **92:**8478–8482

Waldegger, S., Barth, P., Raber, G., Lang, F. 1997. Cloning and characterization of a putative human serine/threonine protein kinase transcriptionally modified during anisotonic and isotonic alterations of cell volume. *Proc. Natl. Acad. Sci. USA* **94:**4440–4445

Wang, Q., Hogg, R.C., Large, W.A. 1993. A monovalent ion-selective cation current activated by noradrenaline in smooth muscle cells of rabbit ear artery. *Pfluegers Arch* **423:**28–33

Wehner, F., Sauer, H., Kinne, R.H. 1995. Hypertonic stress increases the Na^+ conductance of rat hepatocytes in primary culture. *J. Gen. Physiol.* **105:**507–535

Weyand, B., Warth, R., Bleich, M., Kerstan, D., Nitschke, R., Greger, R. 1998. Hypertonic cell shrinkage reduces the K^+ conductance of rat colonic crypts. *Pfluegers Arch.* **436:**227–232

Yellen, G. 1982. Single Ca^{2+}-activated nonselective cation channels in neuroblastoma. *Nature* **296:**357–359